

L. Axelsson,<sup>1</sup> M. J. G. Borge,<sup>2</sup> S. Fayans,<sup>3</sup> V. Z. Goldberg,<sup>3</sup> S. Grévy,<sup>4</sup> D. Guillemaud-Mueller,<sup>4</sup> B. Jonson,<sup>1</sup> K.-M. Källman,<sup>5</sup> T. Lönnroth,<sup>5</sup> M. Lewitowicz,<sup>6</sup> P. Manngård,<sup>5</sup> K. Markenroth,<sup>1</sup> I. Martel,<sup>2</sup> A. C. Mueller,<sup>4</sup> I. Mukha,<sup>7</sup> T. Nilsson,<sup>1</sup> G. Nyman,<sup>1</sup> N. A. Orr,<sup>8</sup> K. Riisager,<sup>7</sup> G. V. Rogatchev,<sup>3</sup> M.-G. Saint-Laurent,<sup>6</sup> I. N. Serikov,<sup>3</sup> O. Sorlin,<sup>4</sup> O. Tengblad,<sup>2</sup> F. Wenander,<sup>1</sup> J. S. Winfield,<sup>8</sup> and R. Wolski<sup>9</sup>

<sup>1</sup>Fysiska Institutionen, Chalmers Tekniska Högskola, S-412 96 Göteborg, Sweden

<sup>2</sup>Instituto de Estructura de la Materia, CSIC, E-28006 Madrid, Spain

<sup>3</sup>Russian Scientific Center "Kurchatov Institute", Institute of General and Nuclear Physics, RU-123182 Moscow, Russia

<sup>4</sup>Institut de Physique Nucléaire, IN2P3-CNRS, F-91406 Orsay Cedex, France

<sup>5</sup>Department of physics, Åbo Akademi, FIN-20500 Turku, Finland

<sup>6</sup>GANIL, BP 5027, F-14021 Caen Cedex, France

<sup>7</sup>Institut for Fysik og Astronomi, Aarhus Universitet, DK-8000 Aarhus C, Denmark

<sup>8</sup>Laboratoire de Physique Corpusculaire, Université de Clermont Ferrand II, F-14050 Caen Cedex, France

<sup>9</sup>Joint Institute for Nuclear Research, RU-141980 Dubna, Russia

Resonances in the unbound nucleus  $^{11}\text{N}$  have been studied, using the resonance scattering reaction  $^{10}\text{C}+p$ . The data give evidence for three states above the  $^{10}\text{C}+p$ , threshold with energies 1.30, 2.04, and 3.72 MeV. These states can be interpreted, in a potential-model analysis, as the ground state and the first two excited states with spin-parity  $1/2^+$ ,  $1/2^-$ , and  $5/2^+$  arising from the shell-model orbitals  $1s_{1/2}$ ,  $0p_{1/2}$ , and  $0d_{5/2}$ . A narrow state superposed on a broad structure found at higher energy could be interpreted as the mirror state of the  $3/2^-$  in  $^{11}\text{Be}$  shifted down in energy. This shift would suggest a large radius of the potential.

PACS number(s): 21.10.Pc, 25.40.Ny, 27.20.+n

Spectroscopic information regarding nuclei on the  $A=11$  isobaric chain is, on the neutron-rich side, available for the two exotic nuclides  $^{11}\text{Be}$  and  $^{11}\text{Li}$ . These are examples of the novel structural feature, the neutron halo (see for example [1-3] and references therein), which has attracted considerable interest to nuclei in the drip-line regions. On the proton-rich side, it is known that the nucleus  $^{11}\text{N}_4$  is unbound and the aim of this work is to identify the ground state and excited states in this system. An interesting question in this context is whether  $^{11}\text{N}$  shows the same parity inversion that is observed in  $^{11}\text{Be}$ , in which the ground state is an  $1s_{1/2}$  intruder state and the only bound excited state at 320 keV is a  $0p_{1/2}$  state. Both these states have large single particle spectroscopic factors (SF) to  $^{11}\text{Be}(\text{g.s.})$  [4].

Until recently, the only experimental data available for  $^{11}\text{N}$  had been obtained by Benenson et al. [5] in a study of the reaction  $^{14}\text{N}(^3\text{He},^6\text{He})$ . They observed a resonance state at 2.24 MeV above the  $^{10}\text{C}+p$  threshold with a width of 0.74 MeV. The data gave evidence for a state in  $^{11}\text{N}$  which, through indirect arguments, was interpreted to be the  $1/2^-$  first excited state and not the  $1/2^+$  ground state. Guimarães *et al.* [6] have recently investigated the  $^{14}\text{N}(^3\text{He},^6\text{He})$  reaction and claim that the state observed in [5] is in reality composed of two states. New data have also been obtained [7] from studies of fragmentation of  $^{12}\text{N}$  that indicated the existence of a low-lying state in  $^{11}\text{N}$  at an energy of 1.2 MeV above the  $^{10}\text{C}+p$  threshold.

The main problem in all spectroscopic investigations of nuclei far from stability in general is the necessity of using very complicated reactions in order to reach the exotic nuclei. This is the main reason why many contradictory

results have been obtained. Furthermore it is difficult to get quantum characteristics of the levels, important for any comparison with theories of nuclear structure.

Therefore, a more direct method of studying the resonances in  $^{11}\text{N}$  was selected, namely the resonance scattering reaction  $^{10}\text{C}+p$  in inverse geometry. We found that this simple reaction provides the opportunity to give indisputable spin-parity determinations, energies, and widths of the lowest three states in  $^{11}\text{N}$ . In short, the method consists of a heavy ion beam which enters a scattering chamber via a thin window. The scattering chamber is filled with a gas

The experiment was carried out at the heavy-ion accelerator GANIL in Caen, France. A primary beam of  $^{12}\text{C}$ , with an energy and intensity of 75 MeV/u and  $10^{12}$  pps respectively, was directed onto a  $1.5\text{ g/cm}^2$  thick Be target. From the fragmentation products a secondary beam of  $^{10}\text{C}$ , with kinetic energy of 110 MeV (energy spread  $\Delta E=1.5\text{ MeV}$ ), was extracted using the LISE3 spectrometer [8]. The beam intensity (after a  $220\text{ }\mu\text{m}$  thick Be degrader) was about  $7\cdot 10^3$  pps and the admixtures of protons and  $\alpha$ -particles in the beam were found to be less than  $10^{-8}$  of the  $^{10}\text{C}$  intensity. The  $^{10}\text{C}$  nuclei passed through a parallel plate avalanche counter (PPAC) that, together with the radio frequency from the cyclotron (RF), gave the time of flight for each particle. Then the  $^{10}\text{C}$  beam entered the scattering chamber (Fig. 1) filled with  $\text{CH}_4$ . The gas served as a target and the scattered protons from the reaction  $^{10}\text{C}+p$  were detected in an array of silicon detectors. The gas pressure was tuned in order to stop the  $^{10}\text{C}$  beam completely just in front of the detectors. The basic ideas of the thick-target method

used, as well as its application to radioactive beams can be found in [9] and [10]. A Monte Carlo simulation of the experiment was performed, showing that the full width at half maximum was better than 50 keV above 1.5 MeV (c.m.). As a calibration and test of the set up, a  $^{12}\text{C} + \text{p}$  run was performed with similar conditions as for the  $^{10}\text{C}$  beam. Figure 2 shows the resulting recoil proton energy spectrum measured at  $0^\circ$  in the vicinity of 3.55 MeV excitation energy in  $^{13}\text{N}$ . Two partly overlapping levels in  $^{13}\text{N}$  at 3.50 MeV (62 keV width) and 3.55 MeV (47 keV width) are known in this energy region [11]; the latter being dominant. The precision in energy was obtained from a potential model fit and found to be 20 keV. This was included as a systematic experimental error in the level energies determined for  $^{11}\text{N}$ .

The background from the carbon in the  $\text{CH}_4$  molecules was determined by measurements with  $\text{CO}_2$  gas in the chamber. From this, we estimate that the carbon contributed less than 10% to the total intensity and showed a constant, featureless energy distribution.

Figure 3 shows the  $^{10}\text{C} + \text{p}$  excitation function in the c.m. obtained with the detector mounted at zero degree, corresponding to  $180^\circ$  in c.m. A detailed description of the conversion procedure from raw data to excitation function will be given in a forthcoming paper [12].

The three lowest states in  $^{11}\text{Be}$  are predominantly of single-particle nature with SF's known to be greater than 0.6 [4]. The analysis is based on the assumption that this is also valid for the  $^{11}\text{N}$  case, allowing us to use a potential-well model to generate the resonances observed in  $^{10}\text{C} + \text{p}$  elastic scattering. A central Woods-Saxon potential together with a spin-orbit term, using conventional values of the radius and diffuseness parameters, was utilized. To get the best fit to the data, the depth for each  $\ell$  value was varied. The geometrical parameters of the fit are  $r_0 = 1.2$  fm and  $a = 0.53$  fm. The spin-orbit potential is  $V_{s.o.} = 5.5$  MeV and the Coulomb potential is that of a uniformly charged sphere with  $r_{0C} = r_0$ . For orbital momenta  $\ell$  greater than 2 the well depth was chosen to be constant and equal to the value obtained for  $\ell = 1$ . Because of the small c.m. energy we have not included an imaginary part of the potential.

The calculated excitation function is shown as a full-drawn curve in Fig. 3. The result, assuming levels with the same spin and parity as in  $^{11}\text{Be}$  gives a very good description of the zero-degree experimental data up to 4 MeV (c.m.). The positions and widths of the resonances were evaluated from the resonance behavior of the corresponding partial wave in the potential with parameters fixed by the fit of the experimental excitation function. These are given in Table I and taken as our experimental results. This approach is basically similar to the one used by Fortune et al. [13] and Barker [14] to calculate levels in  $^{11}\text{N}$  and also to what Baz et al. [15] used to describe  $\alpha$ -particle scattering in the vicinity of resonances. The present approach has a clear advantage

over a conventional R-matrix analysis since the number of free parameters is much smaller. Furthermore, it allows a straightforward interpretation and a direct comparison with the  $^{11}\text{Be}$  case.

At higher energies we have used a coherent sum of Breit-Wigner resonances to fit the experimental excitation function (dashed line in Fig. 3). In this regime the solid angle corrections are large and furthermore the thickness of the Si detector cuts the spectra at 5.3 MeV (c.m.). The energies and widths of the resonances are given in Table I. The results in the region above 4 MeV are limited by the sensitivity in our data, and should be considered mainly as an indication of resonances at higher energies. Because of this uncertainty, we did not consider interference effects between the lower and upper parts of the calculated curve.

The level at 3.72 MeV (which appears at 3.6 MeV in the excitation function by interference) is a  $5/2^+$  resonance. A possible  $3/2^+$  assignment could be rejected since it would give a smaller cross section and  $5/2^-$  would result in a much narrower structure. The levels at 1.3 MeV and 2.04 MeV are assumed to have spin  $1/2$ . A  $3/2^-$  resonance would correspond to a much larger cross section and destroy the overall agreement. Furthermore, the same parity for the two resonances in question could be excluded because of the observed interference pattern. The 1.3 MeV resonance is also too broad to be a  $1/2^-$  state. Therefore, the assumptions of the spin-parity assignments incorporated in the calculated curve in Fig. 3 (below 4 MeV) give a reasonably good description of the experimental data and seem to be the only possible choice.

In contrast to the definite conclusions at low energies, the description of the experimental data at energies above 4.0 MeV serves only as a guide, being useful only in the context of a more thorough analysis. In the vicinity of 4.5 MeV, there is a structure that seems to be statistically significant (to a 90% confidence level). This structure attracted our attention mainly because there is a known [4] very narrow (15 keV)  $3/2^-$  level in  $^{11}\text{Be}$  at 3.9 MeV excitation energy. Preliminary data of Guimarães et al. [6] shows a very prominent peak that can be interpreted as a  $^{11}\text{N}$  level in this energy region. According to our supposition based on the  $^{14}\text{N}(^3\text{He}, ^6\text{He})$  reaction mechanism, the level should be a  $3/2^-$  state. We have assumed that this state is the mirror state of the known state in  $^{11}\text{Be}$ . The evaluation of the width (less than 100 keV) and an upper limit of the cross section (200 mb/sr) is then readily done. The broad structure in the high-energy end of the measured excitation function can be assigned as an effect of two broad overlapping levels with spin-parity  $5/2^+$  and  $3/2^+$ . (The known  $^{11}\text{Be}$  data [4] give some basis for this assumption.) For a single state, the observed cross section would definitely yield a spin greater than  $5/2$ . Hence, the high-energy part of the measured distribution is tentatively described as a coherent sum

of three resonances. The data obtained from the detectors mounted off-center (see Fig. 1) were analyzed in the same way and the results (not shown here) were found to fully correspond to the results obtained from the central detector.

As shown in Fig. 3, the "conventional" radius ( $r_0=1.2$  fm) of the potential gives a good description of the experimental excitation function for  $^{11}\text{N}$ . However, when applied to the  $^{11}\text{Be}$  case, it results in systematic overbinding of the states. To get a simultaneous description of the states in the two nuclei, it is necessary to decrease the relative role of the Coulomb interaction. This was done by increasing the radius of the nuclear and Coulomb potential to  $r_0=1.4$  fm, keeping the other geometrical parameters as before. A good fit to the level positions in the two mirror nuclei was then achieved. (The reason why Fortune et al. [13] did not get the right positions of the levels in their calculations is the use of a conventional radius parameter.) The shape of the excitation function obtained with the large radius potential is about the same for the  $s$  and  $p$  states but yields a larger width for the  $d$  state. Taking the potential with the large radius, we obtain the SF's for the unstable states in the  $^{11}\text{N}$  nucleus by comparing with the experimental widths (Table I).

Table II gives the calculated level energies in  $^{11}\text{Be}$  for both sets of parameters used. One still observes an overbinding of the  $0p_{1/2}$  level. This can be understood as an indication of a more pure single-particle character of this state compared to the  $1s_{1/2}$  and  $0d_{5/2}$  states.

Part of the level schemes for  $^{11}\text{Be}$  and  $^{11}\text{N}$  are shown in Fig. 4. One notes that both the  $1/2^+$  ground state and the assumed  $3/2^-$  state are shifted downward in energy relative to the  $5/2^+$  state. The larger shift is found for the  $3/2^-$  state. An explanation for this might be that the structure of this level is a hole in the  $0p_{3/2}$  shell with two particles in the  $1s_{1/2}$  state. Experimentally, this is supported by the narrow width and the large cross section for the  $^9\text{Be}(t,p)$  reaction [4]. Based on this assumption, we should get a relative shift, which is twice as big as for the ground state. This is in good agreement with our observation. A study of this state is an interesting challenge for the future.

In conclusion, we have been able to identify the low-energy states in the unbound nucleus  $^{11}\text{N}$ . The experimental data made the assignments of the quantum characteristics of the three lowest states possible. These states have similar structure as the ground state and the two first excited states in  $^{11}\text{Be}$ . In our comparisons of the level positions, we need to assume that both nuclei have a large radius of the common potential. The SF's obtained for the three lowest states are found to be large which suggests a  $^{10}\text{C}+p$ -like structure of the resonance states.

We are indebted to Professor M.V. Zhukov and Professor F.C. Barker for fruitful discussions. We also acknowl-

edge financial support from the European Community under Contract No. CHGE-CT94-0056 (Human Capital and Mobility, Access to the GANIL large scale facility) and from the Russian Foundation RFFI.

- 
- [1] P.G. Hansen, A.S. Jensen, and B. Jonson, *Annu. Rev. Nucl. Part. Sci.* **45**, 591 (1995).
  - [2] I. Tanihata, *J. Phys. G* **22**, 157 (1996).
  - [3] M.V. Zhukov et al. *Phys. Rep.* **231**, 151 (1993).
  - [4] F. Ajzenberg-Selove, *Nucl. Phys. A* **506**, 2 (1990).
  - [5] W. Benenson et al., *Phys. Rev. C* **9**, 2130 (1974).
  - [6] V. Guimarães et al., in *Physics of Unstable Nuclei Proceedings of the International Symposium on Physics of Unstable Nuclei, Niigata, Japan 1994*, edited by H. Horiuchi et al., Elsevier Science, New York, 1995, p. 161C; *Nucl. Phys. A* **588**, 161C (1995).
  - [7] M. Thoennessen et al., in *Proceedings of the International Conference on Exotic Nuclei and Atomic Masses ENAM-95*, edited by M. de Saint Simon et al. (Editions Frontiers, Gif-sur-Yvette, 1995, p. 237.
  - [8] A.C. Mueller, and R. Anne, *Nucl. Instrum. Methods Phys. Res B* **56**, 559 (1991).
  - [9] K.P. Artemov et al., *Sov. J. Nucl. Phys.* **52**, 1460 (1990).
  - [10] V.Z. Goldberg, and A.E. Pakhomov, *Phys. At. Nucl.* **56**, 1167 (1993).
  - [11] F. Ajzenberg-Selove, *Nucl. Phys. A* **523**, 1 (1991).
  - [12] L. Axelsson et al., to be published
  - [13] H.T. Fortune, D. Koltenuk, and C.K. Lau, *Phys. Rev. C* **51**, 3023 (1995).
  - [14] F.C. Barker, *Phys. Rev. C* **53**, 1449 (1996).
  - [15] A.I. Baz et al., *Lett. Nuovo Cim.* **18**, 227 (1977).

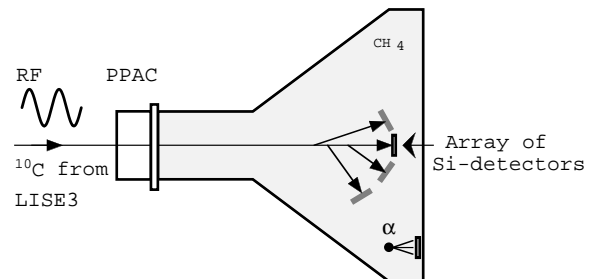


FIG. 1. The experimental arrangement used in the resonance scattering experiment. The beam of  $^{10}\text{C}$ , separated in the LISE3 spectrometer, enters the scattering chamber via an  $80\text{ mg/cm}^2$  kapton window. The target gas is  $\text{CH}_4$  with a pressure chosen to stop the carbon ions in front of the central detector. The scattered protons were detected in an array of Si detectors placed at various angles. The thicknesses of the detectors were between 2-2.5 mm, which allowed measurements of scattered protons up to 15-20 MeV. The gas pressure was measured both with a manometer and indirectly with an  $\alpha$ -particle source placed 4 cm from a Si detector.

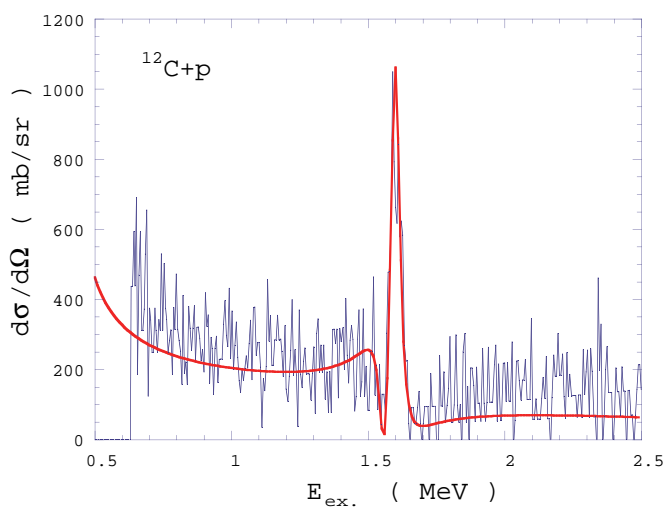


FIG. 2. Part of the excitation function of  $^{12}\text{C}+p$  elastic scattering. The full drawn curve is a potential model fit. The intensity of the  $^{12}\text{C}$  beam was  $10^4$  pps and the measuring time six hours. A 0.001% admixture of  $\alpha$ -particles and  $10^{-5}$  % of deuterons were observed in the beam but with energies above the region shown.

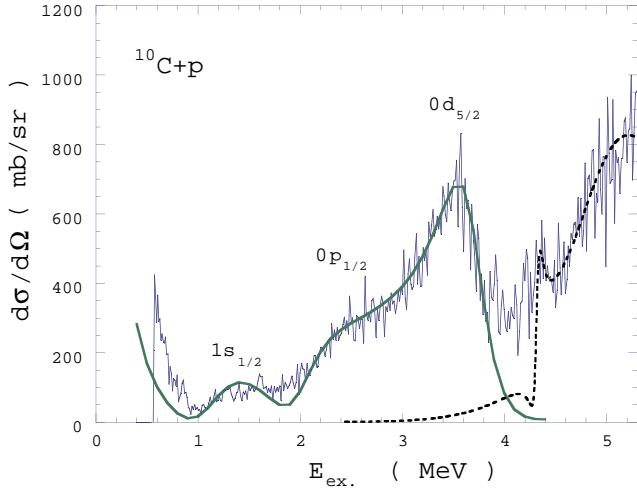


FIG. 3. Part of the excitation function of  $^{10}\text{C}+p$  elastic scattering. The intensity of the  $^{10}\text{C}$  beam was  $7 \cdot 10^3$  pps and the measuring time 16 hours. The full drawn curve shows a potential model fit to the data in the low energy region and the dashed curve is a result of a fit with a coherent sum of Breit-Wigner resonances. The increase of intensity below 1 MeV is a combined effect of Coulomb scattering (fit),  $^{10}\text{C}$  ions not completely stopped in the  $\text{CH}_4$  gas, and background from the decay of  $^{10}\text{C}$ .

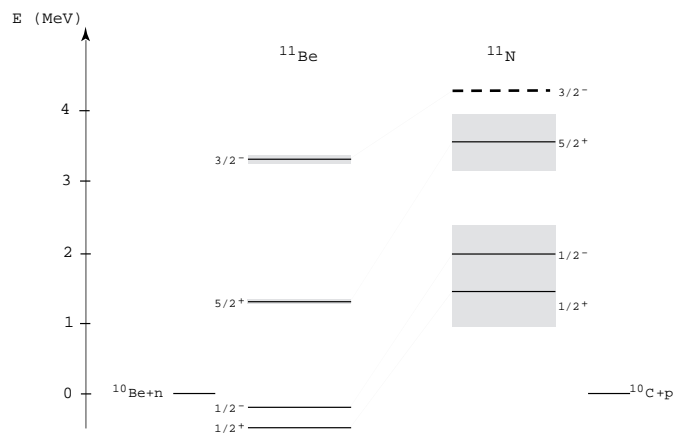


FIG. 4. The lowest energy levels for  $^{11}\text{Be}$  and  $^{11}\text{N}$ .

TABLE I. Levels in  $^{11}\text{N}$ .

Level $I^\pi$	Energy <sup>b</sup> MeV	$\Gamma_{c.m.}$ keV	SF
$1/2^+$	$1.30 \pm 0.04$	$990^{+100}_{-200}$	0.76
$1/2^-$	$2.04 \pm 0.04$	$690^{+50}_{-100}$	0.9
$5/2^+$	$3.72 \pm 0.04$	$600^{+100}_{-40}$	0.73
$3/2^-$ <sup>a</sup>	4.32	70	—
$3/2^+$ <sup>a</sup>	5.1	1100	—
$5/2^+$ <sup>a</sup>	5.5	1500	—

<sup>a</sup>Tentative assignment.

<sup>b</sup>Relative to the  $^{10}\text{C}+p$  threshold.

TABLE II. Levels in  $^{11}\text{Be}$  (MeV).

Level $I^\pi$	Experimental	Calculated ( $r_0=1.4$ fm)	Calculated ( $r_0=1.2$ fm)
$1/2^+$	0	-0.016	-0.146
$1/2^-$	0.320	0.134	-0.086
$5/2^+$	1.779	1.81	1.464